Lineage relationship and protective immunity of memory CD8 T cell subsets

E. John Wherry [1]*, Volker Teichgräber [1]*, Todd C. Becker[1], David Masopust[1], Susan M. Kaech[1], Rustom Antia[2], Ulrich H. von Andrian[3] and Rafi Ahmed[1]

Published online 3 February 2003; doi:10.1038/ni889

Memory CD8 T cells can be divided into two subsets, central (T_{CM}) and effector (T_{EM}), but their lineage relationships and their ability to persist and confer protective immunity are not well understood. Our results show that T_{CM} have a greater capacity than T_{EM} to persist *in vivo* and are more efficient in mediating protective immunity because of their increased proliferative potential. We also demonstrate that, following antigen clearance, T_{EM} convert to T_{CM} and that the duration of this differentiation is programmed within the first week after immunization. We propose that T_{CM} and T_{EM} do not necessarily represent distinct subsets, but are part of a continuum in a linear naive → effector → T_{EM} → T_{CM} differentiation pathway.

Memory T cells are well suited to combat pathogens because they are present at higher numbers than naive cells, they persist for extended periods due to antigen-independent homeostatic turnover and they respond rapidly upon reencounter with pathogen[1]. Two subsets of memory T cells were described based on their anatomical location, expression of cell surface markers and effector functions[2]. Memory T cells that express molecules such as CD62L and CCR7, which allow efficient homing to lymph nodes (LN), are termed central memory cells (T_{CM}), whereas memory T cells that lack expression of these LN homing receptors and are located in nonlymphoid tissues are termed effector memory cells (T_{EM}). However, both T cell subsets are present in the blood and spleen. Some studies have also shown that T_{EM} acquire effector functions, such as cytokine production and killing, more rapidly than T_{CM}[2–4].

The existence of T_{CM} and T_{EM} subsets raises several important questions about memory T cell differentiation and protective immunity. Recently, considerable interest has focused on memory T cell differentiation, but it is unclear how T_{CM} and T_{EM} subsets are generated and whether they represent separate or related lineages. One study examining T cell differentiation *in vitro* showed that T_{CM} and T_{EM} generation can be influenced by cytokines such as interleukin (IL)-2 and IL-15[5]. Based on this study, a model was proposed in which T_{CM} and T_{EM} can arise as separate branches during T cell differentiation[6]. However, the lineage relationship between these two subsets after infection *in vivo* has not been examined. A hallmark feature of memory T cells is the ability to undergo antigen-independent homeostatic turnover and, thus, maintain a stable pool of antigen-specific memory T cells[1,7]. It remains to be determined which memory T cell subset has the greater capacity to persist long-term *in vivo* and undergo homeostatic proliferation. A second defining characteristic of memory T cells is rapid responsiveness to antigen upon secondary infection[1]. T_{EM} may provide a first line of defense in nonlymphoid tissues and therefore may represent a more effective population for protection from reinfection[2], but a direct *in vivo* comparison of the protective capacity of T_{CM} and T_{EM} is lacking.

To examine these questions, we used two well-studied models of T cell immunity, acute infection of mice with lymphocytic choriomeningitis virus (LCMV) or the intracellular bacterium *Listeria monocytogenes* (LM). LCMV and LM represent the prototypical viral and intracellular bacterial pathogens used to study CD8 T cell immunity to intracellular pathogens. Infection with either LCMV or LM results in long-term protective immunity and the generation of a memory CD8 T cell population that is maintained in the absence of antigen[8–11]. Here, we have taken advantage of the P14 transgenic mouse bearing a T cell receptor (TCR) specific for the D^b-restricted LCMV gp33 epitope, as well as a recombinant LM expressing the LCMV gp33 epitope (LMgp33). Our results demonstrate that, following pathogen clearance, there is a linear differentiation path from T_{EM} into T_{CM}, indicating that these memory T cell subsets are part of a continuum of T cell differentiation, rather than separate lineages that arise early during infection. In the absence of antigen, T_{EM} convert directly into T_{CM} and only then gain the ability to undergo efficient homeostatic turnover. The rate at which the T_{EM} to T_{CM} conversion occurs is determined during the first week of stimulation *in vivo* and may depend on the magnitude of the infection. Finally, protective immunity is more efficiently conferred by T_{CM} than T_{EM}, due to the greater proliferative capacity of T_{CM}. Thus, CD8 T cell differentiation after acute infection follows a linear, naive → effector → T_{EM} → T_{CM}, pathway that culminates in the generation of a cell type, T_{CM}, that has acquired the two hallmark characteristic of memory T cells: rapid responsiveness to antigen and the stem-cell–like quality of self-renewal.

[1]*Emory Vaccine Center and Department of Microbiology and Immunology, Emory University School of Medicine, and* [2]*Department of Biology, Emory University, Atlanta, GA 30322, USA.* [3]*Center for Blood Research and Department of Pathology, Harvard Medical School, Boston, MA 02115, USA.* **These authors contributed equally to this work. Correspondence should be addressed to R.A. (email: ra@microbio.emory.edu).*

Results

Effector and memory T cell characterization

Normal B6 mice, as well as P14 transgenic mice expressing a TCR specific for the LCMV Db-gp33 epitope, were used in this study. B6 mice were infected directly with LCMV Armstrong, whereas P14 transgenic chimeras were generated by adoptively transferring naive P14 cells (~7.5 10^4) into naive B6 mice and then infecting these chimeric mice with the Armstrong strain of LCMV[9]. Viral titers in the spleen peaked at approximately 3 days post infection (d.p.i.), and virus was eliminated from all tissues by approximately day 8 (**Fig. 1a** and data not shown; ref. 12). The LCMV-specific CD8 T cell response peaked on days 7–8, underwent a contraction phase between days 8 and 30 and resulted in a memory pool whose numbers remained stable over time[10,11] (**Fig. 1a**). Effector CD8 T cells at the peak of the response were highly cytolytic directly *ex vivo*, but this lytic capacity per cell decreased gradually over time[12] (**Fig. 1b**). The amount of *ex vivo* cytotoxicity correlated well with the intensity of staining for granzyme B protein in D^b-gp33–specific CD8 T cells, which decreased as cells differentiated from effectors, through the contraction phase and into memory cells (**Fig. 1c**). Tissue homing properties also changed during the differentiation of naive CD8 T cells into effectors and finally into memory cells (**Fig. 1d**). Naive CD8 T cells efficiently homed to LN, but not to nonlymphoid sites such as the lung and liver. In contrast, effector CD8 T cells had a reduced ability to localize to LN, but gained the ability to enter nonlymphoid organs. Resting memory T cells retained an enhanced capacity to home to the lung and liver compared with naive cells, but, in contrast to effectors, regained the ability to enter LN. All three populations homed to the spleen equally well. A similar pattern of activation and memory CD8 T cell generation was observed after infection of P14 chimeras with LMgp33[9] (data not shown).

The memory T cell compartment can be divided into T_{CM} and T_{EM} subsets based on the expression of several cell surface molecules such as the LN homing receptors[2,13,14]. Consistent with these reports, we found that LCMV D^b-gp33–specific memory CD8 T cells present in the spleen and peripheral blood mononuclear cells (PBMC) could be readily distinguished based on CD62L and CCR7 (**Fig. 2a,b** and data not shown). One subset, representative of T_{CM}, expressed high amounts of CD62L and CCR7, and the other subset, representative of T_{EM}, expressed low amounts of these two homing molecules. CD27 expression was also useful in distinguishing between these two subsets because T_{CM} cells were mostly $CD27^{hi}$, whereas T_{EM} cells were $CD27^{lo/int}$ (**Fig. 2b**). We also examined expression of several canonical cell surface markers of memory CD8 T cells on these two subsets and found that CD44, CD11a, Ly6C, CD122 and CD132 were highly expressed by both subsets (**Fig. 2c**). Neither subset showed evidence of recent TCR activation and both expressed low amounts of CD25 and CD69 and cell size was not increased (FSC; **Fig. 2c**). Thus, both subsets represented "resting" memory CD8 T cells; the $CD62L^{hi}CCR7^{+}CD27^{hi}$ subset corresponded to what is termed T_{CM}, whereas the $CD62L^{lo}CCR7^{-}CD27^{lo/int}$ subset corresponded to what is called T_{EM}.

T_{CM} and T_{EM} have also been defined by anatomical location. Specifically, T_{CM} localize to LN, whereas T_{EM} are found in nonlymphoid organs[3,4,15]. As expected, D^b-gp33–specific memory CD8 T cells found in LN were $CD62L^{hi}$ T_{CM}, whereas most of those in nonlymphoid tissues were of a $CD62L^{lo}$ T_{EM} phenotype (**Fig. 2d**). Both T_{CM} and T_{EM} subsets were present in the spleen and PBMC (**Fig. 2a** and data not shown). Also, the $CD62L^{hi}$ D^b-gp33–specific T_{CM}, but not the $CD62L^{lo}$ T_{EM}, subset had the capacity to respond to the lymphoid chemokines CCL19 and CCL21 in transwell migration assays (**Fig. 2e**; similar results were observed at multiple chemokine concentrations), consistent with their capacity to localize efficiently to LN *in vivo*.

We next analyzed the functional properties of gp33-specific T_{CM} and T_{EM} cells after peptide stimulation *in vitro*. For these experiments, we used two approaches to obtain memory T cell subsets. T_{CM} and T_{EM} cells were purified from the spleen based on CD62L expression (T_{CM}, 92% pure; and T_{EM}, 97% pure) or T_{CM} from the LN were compared with T_{EM} isolated from the liver (similar results were observed for T_{EM} derived from the lung; data not shown). The ability to produce the antiviral cytokines interferon (IFN)-γ and tumor necrosis factor (TNF)-α was similar for T_{CM} and T_{EM} whether they were derived from the LN, spleen or liver; all populations quickly produced these cytokines (**Fig. 2f,g**). In other words, both T_{CM} and T_{EM} were efficient in producing the effector cytokines IFN-γ and TNF-α upon restimulation. However, only T_{CM} (LN or spleen) were capable of producing IL-2 (**Fig. 2f,g**). Little virus-specific cytotoxicity was detected in 5 h directly *ex vivo* for either T_{CM} or T_{EM}, and neither subset expressed high levels of granzyme B (**Fig. 2h,i**). Granzyme B staining of memory T cells isolated from the liver was below the limit of detection (data not shown). However, both memory T cell subsets were equally capable of rapidly acquiring cytotoxic function upon restimulation with peptide, as equivalent levels of target cell lysis were observed at 12 and 18 h (**Fig. 2h** and data not shown).

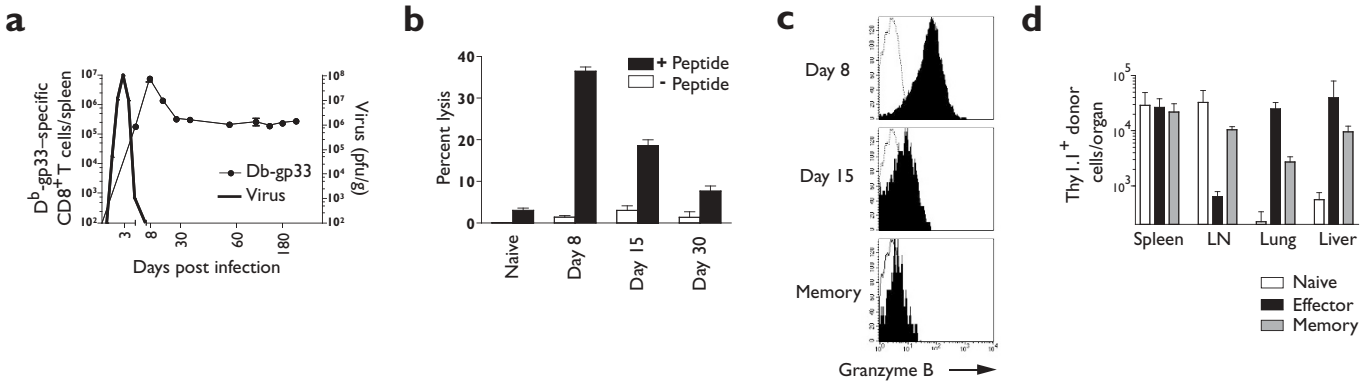

Figure 1. Characterization of effector and memory T cells. (**a**) Viral load and D^b-gp33–specific CD8 T cell numbers in the spleen after LCMV Armstrong infection of B6 mice. (**b**) Cytotoxicity of D^b-gp33–specific CD8 T cells at days 8, 15 and 30 post LCMV Armstrong infection. E:T was 2:1 in all cases. (**c**) Intracellular granzyme B staining of D^b-gp33–specific CD8 T cells at 8, 15 and 125 (memory) d.p.i. The open histogram indicates naive cells. (**d**) *In vivo* homing of naive, effector and memory T cells. Naive, effector (8 d.p.i.) and memory (~60 d.p.i.) P14 cells ($Thy1.1^+$) were adoptively transferred into naive B6 ($Thy1.2^+$) recipients. After 12 h the number of donor ($Thy1.1^+$) gp33-specific CD8 T cells was determined in the indicated organs by flow cytometry.

Thus, the LCMV-specific memory CD8 compartment contained two subsets that resembled T_{CM} and T_{EM}. GP33-specific T_{CM} were $CD62L^{hi}CCR7^{+}CD27^{hi}$, were capable of responding to CCL19 and CCL21, were present in LN, spleen and PBMC and were able to produce IL-2 upon restimulation. T_{EM}, on the other hand, were $CD62L^{lo}CCR7^{-}CD27^{lo/int}$, were less responsive to CCL19 and CCL21, were absent from LN but present in spleen, PBMC and nonlymphoid tissues and did not produce IL-2. However, the canonical memory cell markers CD44, CD11a, Ly6C and CD122 were highly expressed by both subsets. In contrast to some reports[2–4,13,14], but consistent with others[3,16,17], we found that both memory T cell subsets were equally efficient in acquiring effector functions (IFN-γ and TNF-α production and cytotoxicity) upon restimulation with peptide *in vitro*.

Protective immunity by T_{CM} and T_{EM}

We used the following experimental design to address the ability of T_{CM} and T_{EM} to mediate protective immunity (**Fig. 3a**). First, to provide a source of T_{CM} and T_{EM} cells, B6-P14 chimeric mice were infected with LCMV Armstrong or LMgp33[9]. Between 30 and 60 d after resolution of the acute infection, memory T cell subsets were isolated from various tissues of these mice. Then, equal numbers of these memory T cell subsets were adoptively transferred to separate naive recipients and these mice were tested for their ability to control viral infection. Splenic T_{CM} and T_{EM} were purified on the basis of CD62L expression by either flow cytometry or magnetic bead separation (**Fig. 3b**; purity ranged from 80% to 99%). To compare protective capacity of these memory T cell subsets on a per-cell basis, it was critical to demonstrate that the total number of T_{CM} and T_{EM} was the same after adoptive transfer to naive recipients. After transfer, the total number of $CD62L^{hi}$ and $CD62L^{lo}$ memory gp33-specific CD8 T cells recovered from several organs (LN, lung, liver, spleen and bone marrow (BM)) was equivalent (**Fig. 3c**). As expected, T_{CM} homed more efficiently to the LN, whereas T_{EM} had a modest advantage in homing to the lung and liver, confirming the known recirculation properties of these memory T cell subsets[15,18]. Both subsets were equally efficient in homing to the spleen and BM.

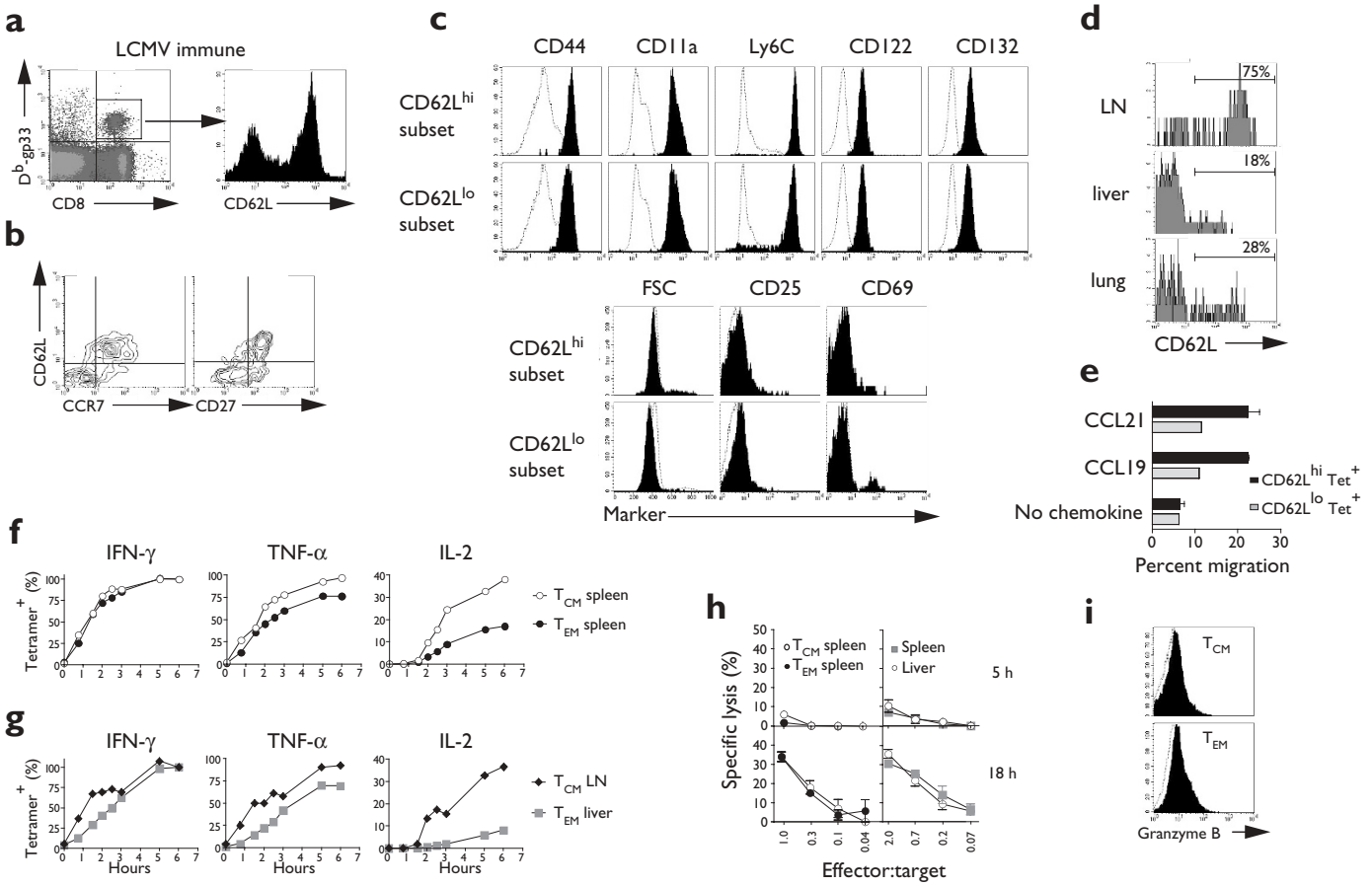

Figure 2. Characterization of memory T cell subsets. (**a**) LCMV D^b-gp33–specific memory CD8 T cells (~2–3 months p.i.) were costained for CD62L expression (histogram is gated on $CD8^+D^b$-$gp33^+$ cells). (**b**) D^b-gp33–specific memory T cells (2–4 months p.i.) were costained for CD62L and CCR7 expression (left) or CD62L and CD27 expression (right). Plots are gated on $CD8^+D^b$-$gp33^+$ cells. (**c**) Phenotypic analysis of $CD62L^{hi}$ and $CD62L^{lo}$ subsets of D^b-gp33–specific memory CD8 T cells. Histograms are gated on either $CD62L^{hi}$ (top) or $CD62L^{lo}$ (bottom) $CD8^+D^b$-$gp33^+$ memory cells (~1–2 months p.i.). Open histograms indicate naive cells. (**d**) LCMV gp33-specific memory (~60 d.p.i.) cells from LN, liver and lung of P14 chimeras were stained for CD62L expression. Histograms are gated $CD8^+D^b$-$gp33^+$ memory cells. Similar results were observed for normal B6 mice. (**e**) Splenocytes from P14 LCMV-immune chimeras (> 30 d.p.i.) were added to a transwell plate and migration in the presence or absence of added chemokine (100 nM) was assessed. (**f**) IFN-γ, TNF-α and IL-2 production by gp33-specific T_{CM} and T_{EM} P14 splenocytes separated using magnetic beads (92% and 97% pure, respectively) was assessed by ICS following gp33 peptide stimulation. (**g**) ICS by T_{CM} from LN and T_{EM} from the liver. (**h**) A 5- and 18-h gp33-specific ^{51}Cr release assay using splenic T_{CM} and T_{EM} purified as in (**f**) (left) or using memory T cells from spleen *versus* liver. All immune mice used in functional experiments were > 30 d.p.i. Background lysis in the absence of gp33 peptide was similar for T_{CM} and T_{EM} and has been subtracted. (**i**) Granzyme B staining of memory T cell subsets from the spleen. T_{CM} are gated on $CD62L^{hi}$ and T_{EM} on $CD62L^{lo}$ D^b-$gp33^+CD8$ T cells at ~60 d.p.i. Open histograms indicate staining with an isotype control antibody.

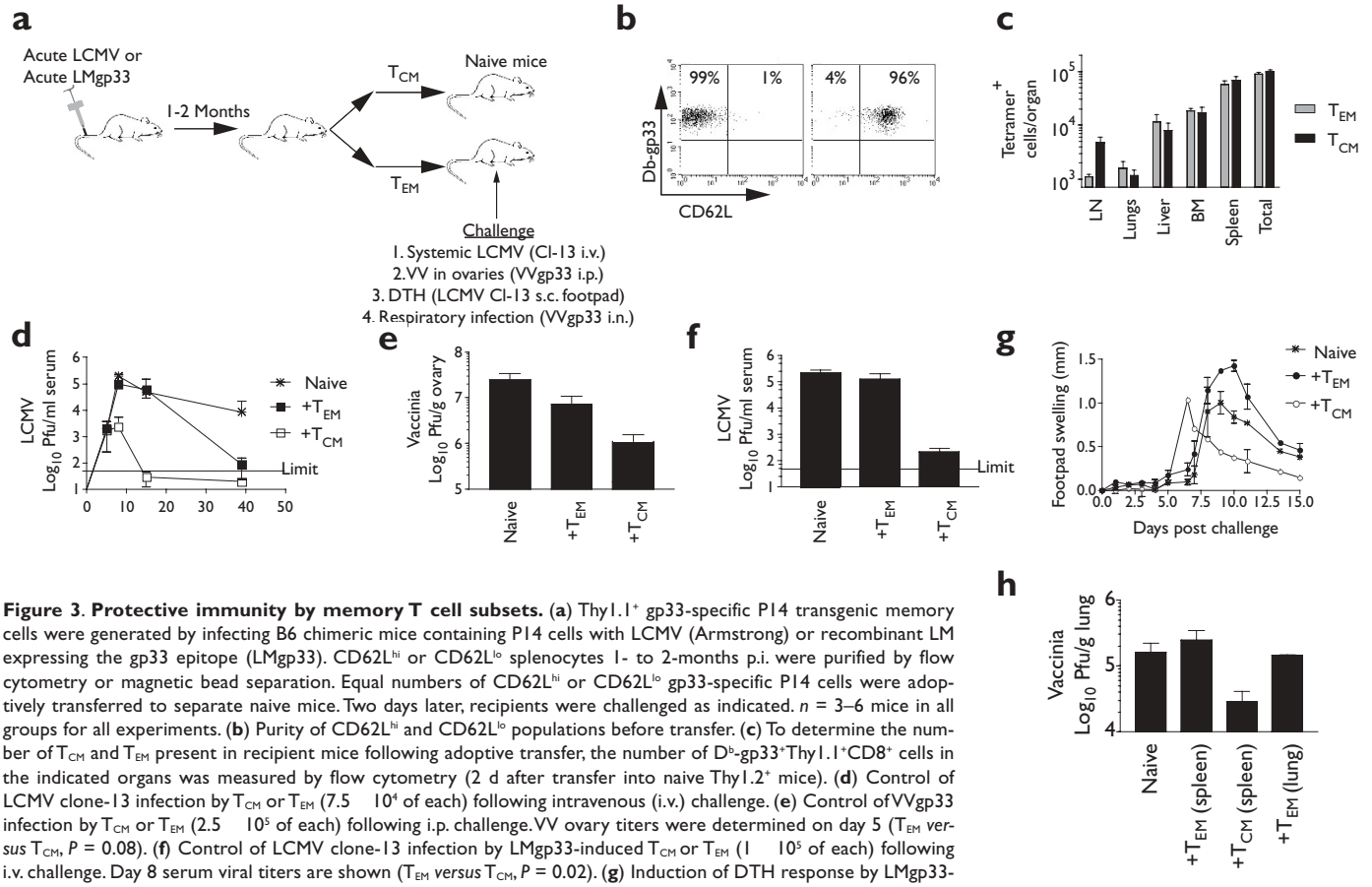

Figure 3. Protective immunity by memory T cell subsets. (**a**) Thy1.1$^+$ gp33-specific P14 transgenic memory cells were generated by infecting B6 chimeric mice containing P14 cells with LCMV (Armstrong) or recombinant LM expressing the gp33 epitope (LMgp33). CD62L^{hi} or CD62L^{lo} splenocytes 1- to 2-months p.i. were purified by flow cytometry or magnetic bead separation. Equal numbers of CD62L^{hi} or CD62L^{lo} gp33-specific P14 cells were adoptively transferred to separate naive mice. Two days later, recipients were challenged as indicated. n = 3–6 mice in all groups for all experiments. (**b**) Purity of CD62L^{hi} and CD62L^{lo} populations before transfer. (**c**) To determine the number of T_{CM} and T_{EM} present in recipient mice following adoptive transfer, the number of D^b-gp33$^+$Thy1.1$^+$CD8$^+$ cells in the indicated organs was measured by flow cytometry (2 d after transfer into naive Thy1.2$^+$ mice). (**d**) Control of LCMV clone-13 infection by T_{CM} or T_{EM} (7.5 10^4 of each) following intravenous (i.v.) challenge. (**e**) Control of VVgp33 infection by T_{CM} or T_{EM} (2.5 10^5 of each) following i.p. challenge. VV ovary titers were determined on day 5 (T_{EM} *versus* T_{CM}, P = 0.08). (**f**) Control of LCMV clone-13 infection by LMgp33-induced T_{CM} or T_{EM} (1 10^5 of each) following i.v. challenge. Day 8 serum viral titers are shown (T_{EM} *versus* T_{CM}, P = 0.02). (**g**) Induction of DTH response by LMgp33-induced T_{CM} or T_{EM} (2 10^5 of each) following footpad injection of LCMV clone-13. Footpad thickness was measured daily. (**h**) Control of VVgp33 infection by LCMV-induced T_{CM}, T_{EM} or lung-derived T_{EM} (3 10^5 of each) following i.n. challenge (T_{EM} spleen *versus* T_{CM}, P = 0.04; T_{EM} lung *versus* T_{CM}, P = 0.003). VV lung titers were determined on day 5. For all protection experiments at least two doses of cells were transferred. The number of memory cells transferred in the experiments shown is indicated in parentheses above.

To evaluate the protective capacity of T_{CM} and T_{EM}, we used four different challenge models that assess viral control by LCMV- or LM-induced memory CD8 T cells. First, after intravenous infection with a virulent strain of LCMV (clone-13), T_{CM} cells mediated considerably more rapid control of a viral infection than did the T_{EM} subset (**Fig. 3d**). Though less effective than T_{CM}, T_{EM} administered to mice caused a more rapid reduction in viremia compared with control mice. Reduced viremia in this model represents viral control in multiple tissues. To examine control of viral replication in a more localized tissue, naive recipients of purified T_{CM} and T_{EM} were challenged intraperitoneally (i.p.) with vaccinia virus (VV) expressing the gp33 epitope (VVgp33) and viral control was examined in the ovary on day 5. T_{CM} again provided better control of viral replication than did the T_{EM} cells (**Fig. 3e**). Thus, whether viral titers were determined in the blood after LCMV clone-13 infection or in a peripheral tissue (ovary) after VV infection, the T_{CM} subset controlled virus more effectively than did T_{EM}. To determine whether memory T cell subsets induced by a different pathogen also displayed similar properties, T_{CM} and T_{EM} were generated by immunization with LMgp33, and purified populations of T_{CM} and T_{EM} were adoptively transferred to naive recipients. These mice were then challenged with LCMV clone-13. Serum viral titers 8 d after systemic LCMV challenge were substantially lower in mice that received T_{CM} than in those that received T_{EM} cells (**Fig. 3f**). T_{CM} also elicited a more rapid virus-specific delayed-type hypersensitivity (DTH) response (**Fig. 3g**) after subcutaneous (s.c.) infection of the footpad with LCMV, demonstrating that T_{CM} could more rapidly initiate a response and accumulate at a site of peripheral challenge than T_{EM}. Thus, whether memory CD8 T cell subpopulations were generated following an acute viral or bacterial infection, T_{CM} consistently demonstrated more effective and rapid pathogen control.

Our next experiment was designed to address protection using an intranasal (i.n.) challenge and to test the capacity of memory T cells derived from a nonlymphoid tissue, the lung, to mediate protection. Spleen-derived T_{CM} or T_{EM} and T_{EM} isolated from the lung (70% CD62L^{lo}) were adoptively transferred and recipients infected i.n. with VVgp33. After 5 d, recipients of T_{CM}, but not T_{EM} (either lung- or spleen-derived), showed significant control of viral replication in the lungs (**Fig. 3h**). In an additional experiment, liver-derived T_{EM} were compared with T_{CM} in their ability to control virus after a systemic LCMV infection and, once again, the T_{CM} cells were superior (data not shown).

These data from the four challenge models showed that T_{CM} more effectively controlled viral replication (either LCMV or vaccinia) on a per cell basis than T_{EM}, irrespective of the route of infection (intravenous, intraperitoneal, intranasal or subcutaneous) or the site of infection (lung, ovary or viremia). This was true whether T_{CM} and T_{EM} were defined phenotypically and purified from the same tissue (splenic CD62L^{hi} CCR7^{hi} *versus* CD62L^{lo} CCR7^{lo}) or defined anatomically and isolated from nonlymphoid tissue (lung or liver). It should also be noted

that these experiments were designed to test the contribution of only the adoptively transferred, gp33-specific T_{CM} or T_{EM} cells to protective immunity, as either highly purified gp33-specific CD8 T cells were transferred or the only shared determinant between the immunizing and challenge pathogen was the gp33 epitope itself (for example, LCMV primed, VVgp33 challenge).

Antigen-driven proliferation of T_{CM} and T_{EM}

What properties endow T_{CM} with greater protective capacity than T_{EM}? Because effector functions were very similar between T_{CM} and T_{EM} (**Fig. 2f–i** and data not shown), we examined the *in vivo* expansion of these subsets after viral challenge. Donor (Thy1.1$^+$) gp33-specific CD8 T cells were enumerated after either systemic or respiratory viral challenge of recipients of T_{CM} or T_{EM}. Five days after systemic challenge, T_{CM} showed greater expansion (two- to five-fold higher frequencies; 2.7- to 4.4-fold greater total numbers/organ) in all tissues examined (**Fig. 4a**). Following respiratory challenge the difference in *in vivo* expansion of T_{CM} and T_{EM} was even more dramatic. T_{CM} recipients contained 10- to 13-fold more virus-specific CD8 T cells in the lung than T_{EM} recipients (**Fig. 4b**). Several recent studies have demonstrated that initial T cell activation *in vivo* occurs in draining LN despite, in some cases, the presence of T cells at the site of inoculation[19–21]. Therefore, it is likely that the greater expansion of T_{CM} cells after infection is a reflection of their ability to localize to the LN. However, it is also possible that the T_{CM} cells have a stronger intrinsic capacity to proliferate following antigenic stimulation than T_{EM} cells. To directly test this hypothesis, we stimulated D^b-gp33–specific T_{CM} or T_{EM} *in vitro* with gp33 peptide and analyzed cell division by division by carboxyfluorescein succinimidyl ester (CFSE) dilution (**Fig. 4c**). T_{CM} showed more proliferation than T_{EM}, indicating that T_{CM} have an inherent proliferative advantage over T_{EM} following antigenic stimulation. Thus, it is likely that the substantially greater expansion of T_{CM} *in vivo* after infection is due to both their inherent capacity to proliferate and their ability to localize to the LN.

We next examined the phenotype of transferred T_{CM} and T_{EM} in several tissues after infection (**Fig. 4d**). Each transferred population was greater than 95% CD62L^{hi} or CD62L^{lo} at the time of transfer (**Fig. 4d**, pre-challenge). As expected, when CD62L^{lo} T_{EM} cells were transferred they remained CD62L^{lo} after infection (left column). However, when CD62L^{hi} T_{CM} cells were transferred, nearly 90% of all gp33-specific CD8 T cells in the spleen, PBMC and liver had become CD62L^{lo} by 5 d.p.i. Even in the LN, approximately 65% of the gp33-specific memory cells were CD62L^{lo}. Similar results were observed following respiratory challenge (data not shown). This conversion from CD62L^{hi} to CD62L^{lo} required reexposure to antigen because cells recovered from all organs after adoptive transfer in uninfected mice maintained their pre-transfer phenotype. In the absence of infection, transferred T_{CM} in the spleen, LN, liver and lung remained 94%, 91%, 82% and 84% CD62L^{hi}, respectively (data not shown). Collectively, these results show that, following antigen challenge, T_{CM} can rapidly convert to CD62L^{lo} effector cells and that T_{CM}-derived secondary effectors can efficiently localize to nonlymphoid tissues including the site of infection. Thus, the major difference in T_{CM} and T_{EM} seems to be not a difference in immediate effector functions (both subsets were equally good), but rather a difference in the ability of T_{CM} to rapidly proliferate and expand after reencountering antigen.

In vivo persistence and lineage relationship

One of the cardinal properties of memory T cells is their long-term, antigen-independent persistence[22–25]. Given the different properties of T_{CM} and T_{EM}, it is important to determine which population persists for extended periods and to understand the lineage relationship between these subsets. The total number of gp33-specific memory T cells in the spleen remained constant between 1 and 3 months post infection (p.i.) with LCMV (**Fig. 5a**) and were stably maintained even at 400 d.p.i. (data not shown). However, during this time the absolute number of T_{EM} cells declined, whereas the number of T_{CM} cells increased proportionally (**Fig. 5a**, top). At very late time points (for example, day 400) ≥95% of the LCMV-specific memory CD8 T cells were CD62L^{hi} (data not

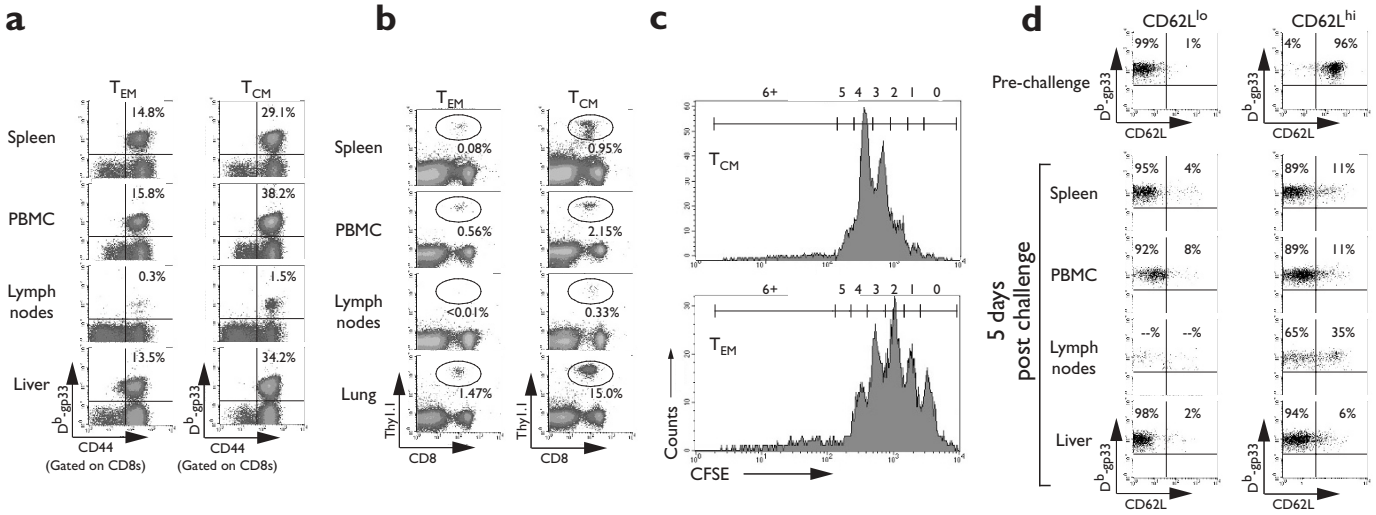

Figure 4. Antigen-driven proliferation of memory T cell subsets. (**a**) *In vivo* T cell expansion following systemic challenge. D^b-gp33$^+$CD8$^+$ T cells were enumerated in spleen, PBMC, LN and liver of T_{CM} and T_{EM} recipients 5 d after i.p. VVgp33 challenge (**Fig. 3e**). All D^b-gp33$^+$CD8$^+$ T cells were donor derived (Thy1.1$^+$; data not shown). T_{CM} recipients had significantly more total Thy1.1$^+$D^b-gp33$^+$CD8$^+$ T cells in all locations examined ($P < 0.05$). (**b**) *In vivo* T cell expansion following respiratory challenge. Thy1.1$^+$ (donor) D^b-gp33$^+$CD8$^+$ T cells were enumerated in spleen, PBMC, LN and lung of T_{CM} and T_{EM} recipients 5 d after i.n. VVgp33 challenge (**Fig. 3h**). T_{CM} recipients had significantly more total Thy1.1$^+$D^b-gp33$^+$CD8$^+$ T cells in lung, spleen and PBMC ($P < 0.05$). (**c**) *In vitro* proliferation of T_{CM} and T_{EM} P14 cells in response to gp33 peptide. The mean division number for T_{CM} and T_{EM} was 3.4 and 2.0, respectively. No division was observed in the absence of gp33 peptide (data not shown). (**d**) Five days after i.p. VVgp33 challenge, recipients of T_{CM} or T_{EM} were sacrificed and the expression of CD62L on secondary effectors in the spleen, PBMC, LN and liver was assessed by flow cytometry. The phenotype of the pretransfer populations of gp33-specific memory cells are shown at the top. Data are representative of 3–4 mice/group.

shown). A similar trend was also observed for CCR7 expression (**Fig. 5a**, bottom) and CD27 expression (data not shown). This pattern of the number of T_{EM} cells decreasing and the number of T_{CM} cells increasing was seen in both the spleen and PBMC. This suggested that either death of the T_{EM} subset was compensated by a reciprocal increase in the T_{CM} population or there was conversion of T_{EM} to T_{CM}. To investigate this issue, gp33-specific memory CD8 T cells were again separated into T_{CM} and T_{EM} on the basis of CD62L and adoptively transferred into naive recipients (**Fig. 5b**). After 25 d the transferred CD62L^{hi} T_{CM} population remained uniformly CD62L^{hi}, but approximately half of the transferred CD62L^{lo} T_{EM} cells had converted to CD62L^{hi} cells, demonstrating that the T_{CM} subset can arise directly from T_{EM} (**Fig. 5b**).

A principal attribute of memory T cells is their ability to undergo homeostatic proliferation to maintain their numbers[23–35]. To examine homeostatic proliferation of memory T cell subsets, purified T_{CM} and T_{EM} were labeled with CFSE and transferred to naive mice (nonirradiated). Thirty days later the division profile of the transferred cells revealed that T_{CM} cells had undergone more divisions (69% divided) compared with T_{EM} cells (36% divided; **Fig. 5c**). As our data (**Fig. 5b**) suggested that the T_{EM} population may give rise to T_{CM}, we next examined the phenotype of CFSE-labeled transferred T_{CM} and T_{EM} cells during homeostatic division. One day after adoptive transfer of purified T_{CM} and T_{EM}, each population maintained its phenotype and, at this early time point, no cell division had occurred (**Fig. 5d**). By

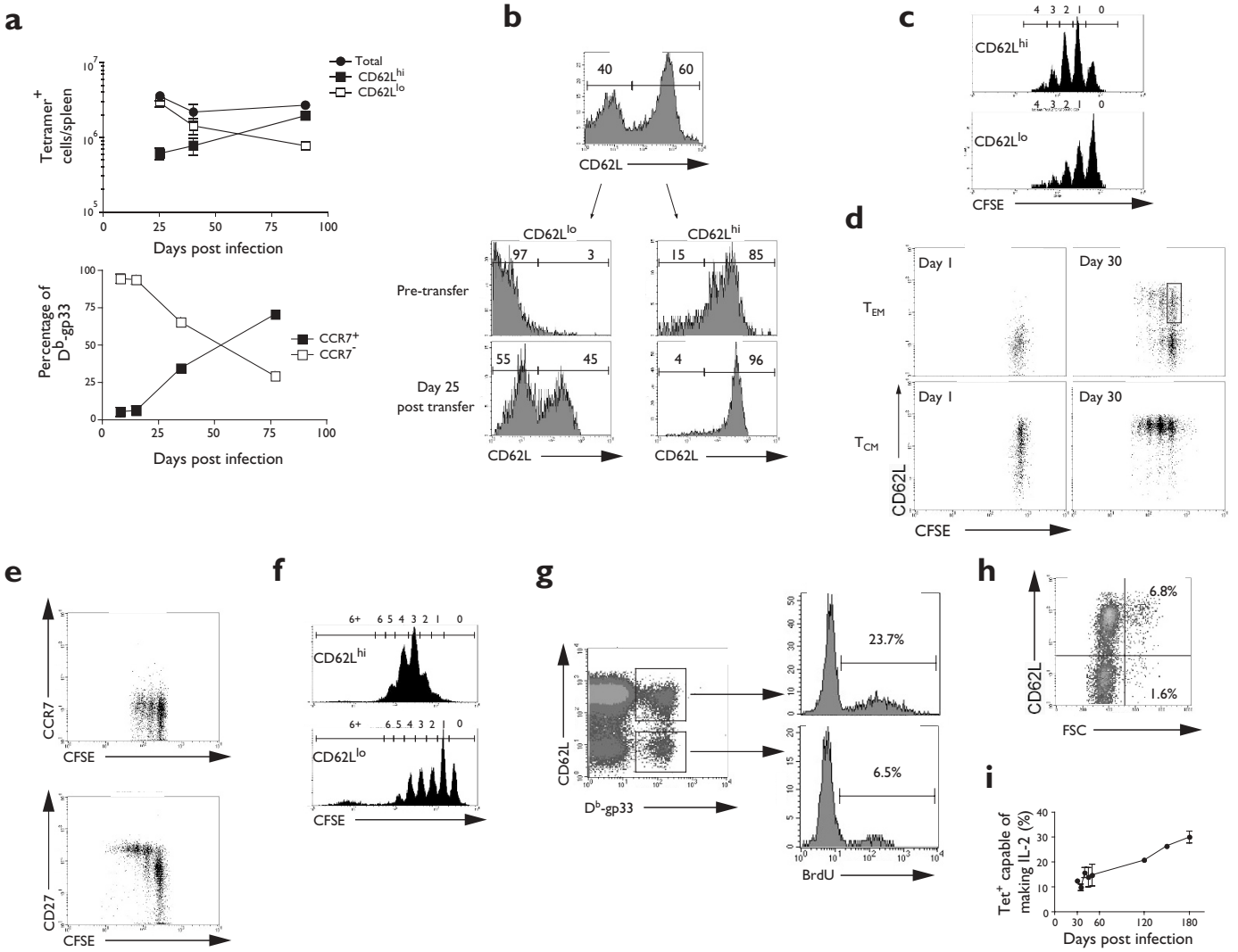

Figure 5. Lineage relationship between memory T cell subsets. (**a**) The number of total and CD62L^{hi} and CD62L^{lo} memory D^b-gp33$^+$CD8$^+$ T cells and the percentage of CCR7$^+$ and CCR7$^-$ D^b-gp33$^+$ CD8 T cells in the spleens of LCMV immune P14 chimeric mice are plotted over time. n = 2–4 mice/time point. (**b**) Column-purified CD62L^{hi} or CD62L^{lo} D^b-gp33$^+$ memory T cells were adoptively transferred into separate naive mice. After 25 d, CD62L expression on splenic D^b-gp33$^+$CD8$^+$ T cells of recipients was determined. (**c**) Purified T_{CM} and T_{EM} cells were CFSE-labeled and transferred into separate naive recipients (nonirradiated). Division of the transferred Thy1.1$^+$ P14 memory cells was assessed after 30 d. (**d**) Purified T_{CM} or T_{EM} D^b-gp33$^+$ cells were CFSE labeled and transferred to naive mice (nonirradiated). After 1 and 30 d, CD62L expression was examined as a function of division. Dot plots are gated on Thy1.1$^+$ P14 memory CD8 T cells from the spleen. (**e**) CCR7 and CD27 expression was examined as a function of cell division on transferred T_{EM} cells 30 d post transfer. (**f**) Purified T_{CM} and T_{EM} D^b-gp33$^+$ CFSE-labeled memory CD8 T cells were transferred separately into naive irradiated recipients. Division of the transferred Thy1.1$^+$ P14 memory cells was analyzed after 8 d. (**g**) LCMV immune (~85 d.p.i.) mice were fed BrdU in their drinking water for 8 d and splenocytes were stained for BrdU incorporation. D^b-gp33 tetramer staining versus CD62L is shown for gated CD8 cells. Histograms are gated on D^b-gp33$^+$CD8$^+$CD62L^{hi} (top) or CD62L^{lo} (bottom) memory T cells. (**h**) D^b-gp33$^+$CD8$^+$ memory T cells (~30 d.p.i.) from a P14 chimera were stained for CD62L expression and the percentage of cells increased in size was indicated by high forward scatter was assessed. Plots are gated on D^b-gp33$^+$CD8$^+$ cells. (**i**) IL-2 production by D^b-gp33–specific memory CD8 T cells was assessed at the indicated times p.i. by intracellular cytokine staining following gp33 peptide stimulation.

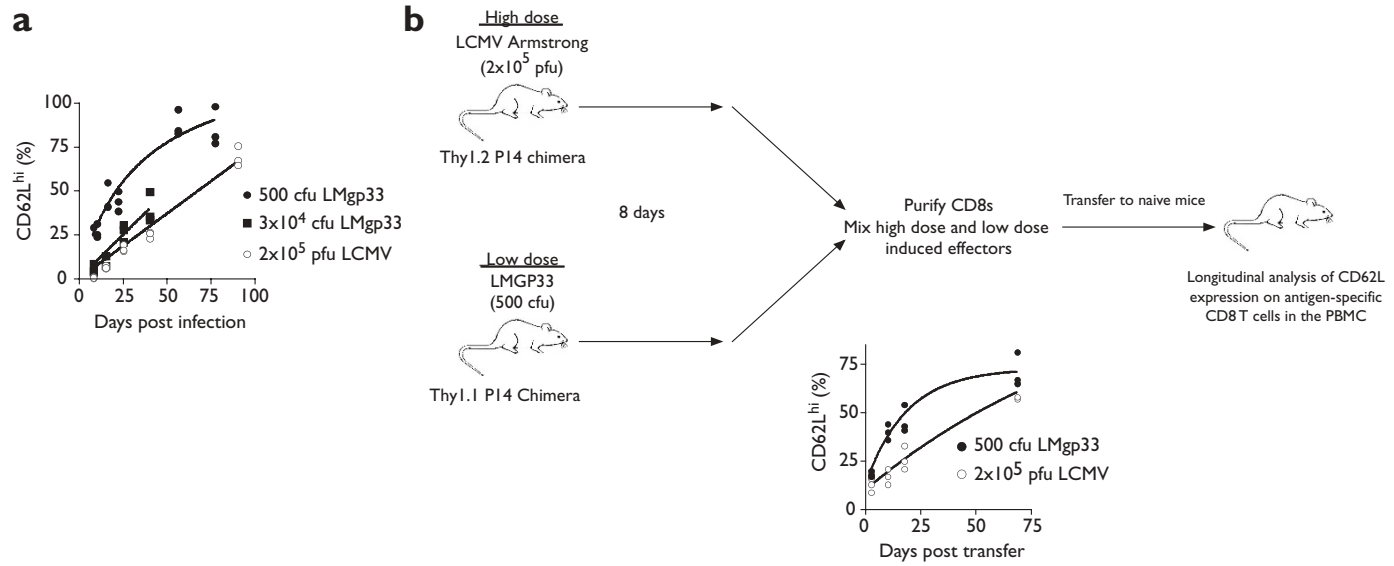

Figure 6. The effect of HD *versus* LD infection on the duration of T_{EM} to T_{CM} conversion. (**a**) P14 chimeras were infected with a LD (500 c.f.u.) or HD (3 10⁴ c.f.u.) of LMgp33 or with LCMV and the percentage of gp33-specific CD8 T cells (P14 cells) that were $CD62L^{hi}$ or $CD62L^{lo}$ in the blood was determined longitudinally in individual mice. (**b**) Naive Thy1.1⁺ P14 chimeras were infected with LD LMgp33 and separate naive Thy1.2⁺ P14 chimeras were infected with LCMV. After 8 d.p.i. spleens were harvested, CD8 T cells column purified (both > 96% pure) and CD8 T cell populations from LMgp33 and LCMV infected mice mixed and transferred into the same recipients. Reexpression of CD62L was monitored on LD LMgp33-induced (Thy1.1⁺) and HD LCMV-induced (Thy1.2⁺) P14 cells parked in the same mice. P14 cells in the PBMC were analyzed over time. Data are representative of four independent experiments.

day 30 post transfer the T_{CM} population had undergone efficient homeostatic proliferation and also retained its phenotype ($CD62L^{hi}$; **Fig. 5d**). These cells also remained $CCR7^{hi}$ and $CD27^{hi}$ (data not shown). In contrast, T_{EM} cells again showed a phenotypic change and by day 30 a substantial proportion (~42%) of T_{EM} cells had converted to $CD62L^{hi}$—it was predominantly this population that had divided (**Fig. 5d**). At day 1 post-transfer there were very few, if any, $CD62L^{hi}$ cells in the T_{EM} population but on day 30 there were a substantial number of memory T cells that had not yet divided but had already converted to $CD62L^{hi}$ (**Fig. 5d**, box). This shows that the emergence of $CD62L^{hi}$ T_{CM} cells from the $CD62L^{lo}$ T_{EM} population truly represents a conversion of the two subsets and is not simply due to proliferation of a few contaminating T_{CM} cells in the purified T_{EM} population. This $T_{EM} \rightarrow T_{CM}$ conversion was also accompanied by increased CCR7 and CD27 expression (**Fig. 5e**). Similar results were observed in multiple tissues (data not shown). These results demonstrate that long-term persistence of memory T cells is primarily in the form of T_{CM}. Further, the T_{EM} subset does not seem to be a permanent memory population, but rather converts to T_{CM} and in so doing acquires the ability to undergo efficient, antigen-independent, homeostatic proliferation. This advantage of T_{CM} in proliferative renewal was confirmed using three additional approaches. Purified T_{CM} and T_{EM} were CFSE labeled and adoptively transferred to naive irradiated recipients in which, after 8 d, substantially more division was observed by the transferred T_{CM} than T_{EM} cells (**Fig. 5f**). Additionally, bromodeoxyuridine (BrdU) labeling was used to analyze memory cell turnover in an unmanipulated mouse (that is, no adoptive transfer). Gated $CD62L^{hi}$ gp33-specific T_{CM} contained ~24% $BrdU^{+}$ cells after one week of BrdU pulse compared with only 6.5% for T_{EM} cells (**Fig. 5g**). Finally, high forward scatter can be used to identify T cells that are currently, or have recently been, in cycle[36]. The D^{b}-gp33–specific T_{CM} subset contained approximately four-fold higher frequency of cells with high forward scatter than the T_{EM} population (**Fig. 5h**).

Thus, during this memory T cell differentiation not only does the expression of LN homing receptors convert from $CD62L^{lo}CCR7^{-}$ to $CD62L^{hi}CCR7^{+}$, but the memory pool also acquires both homeostatic and antigen-driven proliferative potential. A third functional quality of T_{CM} is the ability to produce IL-2 after antigenic stimulation. To test whether this functional property also changed during this memory T cell differentiation, the ability of the memory T cell population to produce IL-2 was examined over time. The proportion of the memory pool capable of IL-2 production gradually increased consistent with an accumulation of T_{CM} cells in the memory pool (**Fig. 5i**). These results demonstrate that, over time, the memory T cell pool converts both phenotypically and functionally from a T_{EM} population that is $CD62L^{lo}CCR7^{-}$, has reduced antigen-driven and little homeostatic proliferative potential and does not produce IL-2 to a T_{CM} subset that is $CD62L^{hi}CCR7^{+}$, proliferates vigorously to antigen, is capable of efficient homeostatic proliferation and has gained the ability to make IL-2 following antigen stimulation.

Programmed $T_{EM} \rightarrow T_{CM}$ conversion rate

We next determined if the differentiation from T_{EM} to T_{CM} was affected by the magnitude of the infection and the duration of antigenic stimulation *in vivo*. We used conditions of low dose (LD) and high dose (HD) immunization that resulted in relatively short (2–3 d) or more prolonged (at least 5–7 d) exposure to antigen. After infection with a LD (500 colony-forming units (c.f.u.)) of LMgp33, antigen can be detected for only 48–72 h[9]. In contrast, following HD (3 10^4 c.f.u.) LMgp33 or LCMV infection, antigen can be detected for at least 5–7 d[9] (unpublished data). P14 chimeric mice were immunized with either a LD or HD of LMgp33, or with an alternative HD with 2 10^5 p.f.u. LCMV (Armstrong). The rate of reversion of gp33-specific T cells from $CD62L^{lo}$ to $CD62L^{hi}$ was monitored in the PBMC of individual mice over time (**Fig. 6a**). The reversion from T_{EM} to T_{CM} occurred much more rapidly in LD immunized mice compared with the HD immunized group. To investigate whether this property of reversion was programmed during the phase of initial

T cell priming or was a result of persisting antigen or the environment, mice containing Thy1.2$^+$ P14 cells were immunized with LCMV (HD) and a separate group of mice containing Thy1.1$^+$ P14 cells was immunized with LD LMgp33 (**Fig. 6b**). On day 8 p.i., effector CD8 T cells were purified from each group, mixed and adoptively transferred to naive recipients. If a low amount of persisting antigen in HD infected mice or the environment was responsible for the slower conversion after HD infection, then after mixing the LD and HD primed effector CD8 T cells and transferring them to a new naive recipient, the two cell populations should both revert at the same rate. If, however, the $T_{EM} \rightarrow T_{CM}$ conversion was programmed during the period of initial T cell priming, then the rate of reversion of HD- and LD-primed T cells parked in the same recipient should remain as observed in the original mice. The results of our experiment were consistent with the latter model. The conversion rate of the LD- and HD-primed cells in the mixed recipients was nearly identical to that observed in the original mice; that is, the HD effectors still reverted slowly and the LD effectors reverted quickly (**Fig. 6b**).

Discussion

There has been considerable interest in understanding the developmental pathways of memory T cells[1,5,6,9,37–43]. The results of our study now allow us to propose a model of T cell differentiation that incorporates the recently defined memory T cell subsets[2]. The essence of this model is that T_{EM} are a transitory population representing an "intermediate" cell type in the effector-to-memory transition. Thus, according to this model, T_{CM} and T_{EM} cells are not distinct subsets but are part of a continuum that ends with the development of T_{CM} cells. T_{CM} are the "true" memory cells because it is only this population that exhibits both of the two hallmark characteristics of memory T cells; long-term persistence *in vivo* by self-renewal and the ability to rapidly expand upon reencounter with pathogen. This model also predicts that memory development is a gradual process and that memory cells only develop several weeks after clearance of the acute infection. Our recent data analyzing global gene expression patterns during memory T cell development are consistent with this model of progressive differentiation[44]. Our study also shows that the rate at which a T cell population converts from $T_{EM} \rightarrow T_{CM}$ can vary depending on the nature of the immunization (high antigen dose versus low antigen dose), and that this conversion rate is programmed during the initial period of encounter with antigen *in vivo*. A strong initial antigenic stimulus imprinted a $T_{EM} \rightarrow T_{CM}$ differentiation program that occurred over several months, whereas a lower amount of priming antigen resulted in more rapid differentiation of T_{EM} to T_{CM}. Thus, the duration of $T_{EM} \rightarrow T_{CM}$ conversion is not constant, but is imprinted during effector generation and varies depending on the magnitude of the initial stimulation.

Our results demonstrate that both T_{CM} and T_{EM} can rapidly elicit effector functions *in vitro* and can both become effectors *in vivo* following reinfection. However, our results also demonstrate that T_{CM} convert to effectors and subsequently to T_{EM} only in the presence of antigen. We found no evidence for T_{CM} converting to T_{EM} in the absence of antigen—even in nonlymphoid tissues after adoptive transfer. While this does not formally exclude that in some locations (such as the intestinal mucosa) or in response to some cytokines an antigen-independent $T_{CM} \rightarrow T_{EM}$ reversion may occur, our results suggest that this reversion back to effectors or T_{EM} is primarily an antigen-driven process.

Many characteristics of T cells change as they differentiate from naive cells to effectors and subsequently to memory cells[44]. Our results demonstrate that this differentiation process continues long after infection has been resolved as T_{EM} convert to T_{CM}. During this $T_{EM} \rightarrow T_{CM}$ conversion memory T cells gradually acquire the ability to undergo efficient homeostatic turnover and to rapidly respond to antigen, and gain the ability to produce IL-2. In contrast, effector-like qualities such as granzyme B expression and the ability to rapidly kill *ex vivo* are lost during the $E \rightarrow T_{EM} \rightarrow T_{CM}$ transition. During this differentiation process hallmark phenotypic changes also occur, some of which (such as CD62L and CCR7 reexpression) affect homing and recirculation properties[15,18,45–47]. Effector cells have an increased capacity to migrate to nonlymphoid tissues, but do not home to LN following adoptive transfer[15,48]. During the transition from effector to memory cells, the ability to migrate to nonlymphoid sites is reduced, though it is still much greater than for naive T cells, but these cells regain the ability to enter LN, a property mainly of T_{CM}. It is likely that the various functional and phenotypic characteristics that change during the $E \rightarrow T_{EM} \rightarrow T_{CM}$ transition do so at different rates. For example, *ex vivo* lytic activity and granzyme B expression are lost before conversion from CD62L^{lo} to CD62L^{hi} or acquisition of the ability to produce IL-2. A key component of this $N \rightarrow E \rightarrow T_{EM} \rightarrow T_{CM}$ model of progressive differentiation is that these qualitative changes occur gradually as the memory population converts to T_{CM}. The ultimate outcome is the formation of a memory population with all of the characteristic properties of a self-renewing, antigen-responsive T_{CM}.

Several recent studies have proposed lineage relationships between memory T cell subsets based on the phenotypic analysis of T cells from human PBMC and analyses of T cells restimulated *in vitro*[2,6,16,41,49,50]. Although these reports provide valuable information characterizing human T cell populations and on the antigen-driven conversion of memory T cells into effectors, it is difficult to draw conclusions about the differentiation of memory T cells *in vivo* from such experiments. Our study has two advantages over these approaches. First, the timing and duration of antigen exposure are known. After acute LCMV or LM infection, antigen is eliminated in approximately 1 week[9,12] and the memory T cells examined several months later have been differentiating in the absence of antigen for a defined period. In the studies analyzing human T cell responses to persisting viruses such as EBV, CMV or HIV, the frequency and amount of stimulation with antigen can vary considerably. Not only do these viruses differ substantially in their level of viral load, but there can also be considerable variation among different individuals. Without precise information about antigen levels, it is difficult to determine whether the memory T cells being analyzed are going through an antigen-independent process of $E \rightarrow T_{EM} \rightarrow T_{CM}$ differentiation that is likely to occur after acute infections or antigen-driven $T_{CM} \rightarrow E$, or $T_{EM} \rightarrow E$ activation of memory T cells. Thus, T cell populations in the PBMC specific for persisting viruses may contain one population of T cells that has not encountered antigen for several days or weeks and another that has been recently exposed to antigen, resulting in a mixture of recently generated effector cells and T_{EM} and T_{CM} cells. The second advantage of our study is that the differentiation of a labeled (Thy1.1$^+$ and/or CFSE-labeled) memory CD8 T cell population was tracked *in vivo*. Such longitudinal studies are essential for defining lineage relationships between different cell populations. Using this approach, the lineage relationship between T_{EM} and T_{CM} *in vivo* was directly demonstrated in our studies. In contrast to previous proposals based on *in vitro* studies[2,6,50], our results demonstrate that the T_{EM} subset is not continually replenished from T_{CM} in the absence of antigen, but rather that T_{CM} cells undergo this differentiation primarily as a result of reencounter with antigen.

Thus, the findings of our study and the proposed model of linear differentiation ($N \rightarrow E \rightarrow T_{EM} \rightarrow T_{CM}$) are likely to provide the paradigm for acute infections. We propose that this will be the natural course of

memory T cell differentiation in the absence of antigen. It is possible, however, that under certain conditions[5,40], especially chronic infections where antigen persists at high amounts[16,49], one may see a different pattern of memory T cell differentiation. Perhaps in these circumstances T cells are caught in a cycle of transition between effector cells and T_{EM}. This could ultimately lead to terminal differentiation, as has been proposed[16] or exhaustion and/or deletion[51,52].

One of the findings of this study was that, on a per-cell basis, T_{CM} controlled systemic and even peripheral or mucosal challenge infections substantially better than did T_{EM}. The enhanced protection by T_{CM} cells did not correlate with a difference in effector functions, as both T_{CM} and T_{EM} (defined both phenotypically and anatomically) produced the effector cytokines IFN-γ and TNF-α rapidly and also quickly acquired CTL function upon reexposure to antigen. Rather, more effective protective immunity by T_{CM} was likely a result of greater expansion of this subset after infection. This greater expansion is at least in part due to an inherent difference in proliferative capacity of T_{CM} and T_{EM}. This may be related to IL-2 production by T_{CM} or may represent additional developmental changes that favor rapid proliferation. Localization of T_{CM} to LN *in vivo* may provide an additional advantage to this subset because dendritic cells efficiently drain from infected sites to LN[53] and *in vivo* T cell responses seem to be initiated in draining LNs rather that at the site of primary infection—even in the presence of tissue resident memory T cells[19–21]. The proliferative advantage of T_{CM} is therefore likely the result of a combination of intrinsic differences in proliferative potential and more efficient antigen presentation *in vivo*.

It should be noted that in all of the challenge models tested in this study, proliferation of antigen-specific CD8 T cells was necessary for efficient pathogen control. In some circumstances, for example after a LD infection in which pathogen control can be achieved without substantial expansion of antigen-specific memory T cells, T_{EM} cells present at the site of initial infection may be more efficient than T_{CM} cells in protective immunity. However, in many instances of protective recall responses, such as vaccine-induced memory T cells responding to a virulent infection, substantial clonal expansion of memory T cells is necessary for efficient pathogen control. Thus, the increased proliferative potential is likely to be one of the most important properties acquired as T_{EM} differentiate into T_{CM}.

The findings of this study have implications for vaccination, especially in terms of determining the optimal time for boosting. Because T_{CM} cells proliferate substantially better than T_{EM} cells upon reexposure to antigen, our results suggest that one should wait until a sufficient number of memory cells have acquired the T_{CM} phenotype before giving the booster immunization. Also, the optimal time interval between the first and second immunization is likely to vary depending on the strength of the primary vaccination. Based on our results, we would predict that stronger vaccines will require a longer interval between the "prime" and "boost" than weaker vaccines. A kinetic analysis of the rate of $T_{EM} \rightarrow T_{CM}$ conversion in the blood after vaccination may allow one to design optimal boosting regimens tailored for individual T cell vaccines. Such an approach would be particularly useful for designing therapeutic vaccination of HIV-infected individuals on antiretroviral therapy. Consistent with this idea, the proliferative capacity of HIV-specific CD8 T cells is significantly greater in long-term nonprogressors who maintain HIV control than in other HIV^+ individuals[54], suggesting that CD8 T cells with strong proliferative potential should be the goal of vaccination approaches.

Methods

Mice, virus and infections. C57BL/6 mice were purchased from The Jackson Laboratory (Bar Harbor, ME). $Thy1.1^+$ P14 mice bearing the D^b-gp33–specific TCR were fully backcrossed to C57BL/6 and maintained in our animal colony[9]. LCMV Armstrong and clone-13 strains, the recombinant *Listeria monocytogenes* (LMgp33) strain and the recombinant vaccinia virus (VVgp33), the latter two of which both express the LCMV gp33 epitope, were propagated, titered and used as described[9,55]. B6 mice were directly infected with LCMV Armstrong (2 10^5 plaque-forming units (p.f.u.) i.p.). P14 chimeric immune mice were generated by adoptively transferring ~5 10^4 to 7.5 10^4 naive TCR transgenic T cells into naive B6 mice followed by LCMV Armstrong infection (these are referred to as P14 chimeras)[9]. Infection of P14 transgenic chimeras with LCMV Armstrong and LMgp33 has been described[9]. All LCMV or LMgp33 immune mice were used at least 30 d.p.i. Mice were challenged with 2 10^6 p.f.u. LCMV clone-13 i.v., 1 10^3 p.f.u. LCMV clone-13 in the footpad (s.c.), or 5 10^6 p.f.u. VVgp33 i.p. or i.n. LCMV stocks were grown and plaque assays performed as described[11]. Vaccinia virus expressing the LCMV gp33 epitope has been described[55]. Vaccinia plaque assays were performed essentially as described for LCMV[11], except after 2.5 d of incubation monolayers were overlayed with crystal violet (0.1% w/v in 20% methanol) and plaques counted. For the footpad challenge, footpad thickness was measured using a Mituoyo Micrometer (Mitutoyo Corporation, Japan). All mice were used in accordance with NIH and the Emory University Institutional Animal Care and Use Committee guidelines.

Isolation of T cell subsets. T_{CM} and T_{EM} were purified by FACS sorting $CD8^+D^b$-$gp33^+CD62L^{hi}$ or $CD8^+D^b$-$gp33^+CD62L^{lo}$ cells. Alternatively, T_{CM} and T_{EM} or total CD8 cells were purified using anti-CD62L or anti-CD8 magnetic beads (Miltenyi Biotec, Auburn, CA) according to the manufacturer's instructions. The purity of FACS-sorted samples (**Fig. 3d**) was 93% for T_{CM} and 95% for T_{EM}, and ranged from 80% to 99% for T_{CM} and T_{EM} purified by magnetic beads. Lymphocytes were isolated from nonlymphoid tissues as described[3,32]. Briefly, mice were euthanized, the hepatic vein cut and 5 ml ice-cold PBS injected directly into the hepatic artery to perfuse the liver, or the left ventricle cut and PBS injected in the right ventricle to perfuse the lungs. Liver or lung tissue was homogenized using a wire screen. Homogenized lung was first incubated in 1.5 mM EDTA at 37 °C for 30 min and both liver and lung were then incubated in 0.25 mg/ml collagenase B (Boehringer Mannheim) and 1 U/ml DNase (Sigma) at 37 °C for 45 min. Digested tissue was applied to a 44/56% Percoll gradient and centrifuged at 850*g* for 20 min at 20 °C. The intrahepatic lymphocyte population was harvested from the interface and red blood cells were lysed using 0.83% ammonium chloride and washed, and the resulting lymphocytes counted. This procedure was found to have little impact on the expression of most cell surface molecules including CD62L (data not shown). Splenocytes isolated in the same manner as liver lymphocytes exhibited similar functional properties to splenocytes isolated by standard procedures (data not shown).

Flow cytometry, intracellular cytokine staining and CTL assays. MHC class I peptide tetramers were made and used as described[11]. All antibodies were purchased from Pharmingen (San Diego, CA). Staining for granzyme B expression was performed using PE-labeled anti-human granzyme B (Caltag, Burlingame, CA). Though a mouse antibody, isotype control staining was low (**Fig. 2i**). The specificity of this reagent was further confirmed by the absence of staining in granzyme $B^{-/-}$ mice (T. Ley, personal communication). CCR7 staining was carried out using CCL19-Ig as described[5]. For intracellular cytokine staining (ICS), lymphocytes (10^6/well) were stimulated with gp33-41 peptide (0.2 g/ml) in the presence of BFA for the indicated periods of time followed by surface staining for CD8 and intracellular staining for IFN-γ, TNF-α or IL-2. ^{51}Cr release assays were performed as described[11], except in all cases the starting E:T ratio was adjusted to obtain identical ratios of D^b-gp33–specific CD8 T cells to target cells for all T cell populations. In addition, the total number of cells/well was kept constant by the addition of naive C57Bl/6 splenocytes. Background cytotoxicity against nonpeptide-pulsed targets was similar for different effector populations and in some cases (**Fig. 2h**) has been subtracted.

Chemotaxis assay. Transwell migration assays were performed as described[56]. Briefly, LCMV-immune splenocytes (3 10^6) from chimeric mice were incubated in the top of a 5 M transwell plate. We added 100 nM, 10 nM or no chemokine to the lower well and cells were incubated at 37 °C for 4 h. Following incubation, lymphocytes were counted in the upper and lower wells and stained for CD8, CD62L and D^b-gp33 tetramer$^+$ memory cells. The percent of the gp33-specific $CD62L^{hi}$ and $CD62L^{lo}$ memory cells added to the upper well that migrated into the lower well was calculated. The chemokines CCL19 (Mip3β) and CCL21 (SLC; 6Ckine) were purchased from R & D Systems (Minneapolis, MN).

Proliferation. Cells were labeled with CFSE (Molecular Probes, Eugene, OR) as described[25]. For *in vitro* proliferation, 1 10^4 of either $CD62L^{hi}$ or $CD62L^{lo}$ D^b-$gp33^+$ cells were cultured in a total of 1 10^6 splenocytes in the presence of 0.2 g/ml gp33 peptide for 60 h. For *in vivo* proliferation, ~1.5 10^5 (irradiated recipients) or 5 10^5 (nonirradiated recipients) CFSE-labeled P14 memory CD8 T cells were adoptively transferred. BrdU labeling and staining were performed as described[25].

Acknowledgments

We thank R. Karaffa for cell sorting; P. Yeiser, K. Madhavi-Krishna and S. Jenkins for technical assistance; T. Ley for help with the granzyme B staining; and E. Ravkov and J.D. Altman

for helpful discussions. Supported by National Institutes of Health grant AI30048 and AI44644 (to R. Ahmed), a Cancer Research Institute fellowship (to E.J.W. and D.M.) and a Damon Runyon-Walter Winchell fellowship (to S.M.K.).

Competing interests statement
The authors declare that they have no competing financial interests.

Received 10 October 2002; accepted 6 January 2003.

1. Kaech, S.M., Wherry, E.J. & Ahmed, R. Effector and memory T-cell differentiation: implications for vaccine development. *Nat. Rev. Immunol.* **2**, 251–262 (2002).
2. Sallusto, F., Lenig, D., Forster, R., Lipp, M. & Lanzavecchia, A. Two subsets of memory T lymphocytes with distinct homing potentials and effector functions. *Nature* **401**, 708–712 (1999).
3. Masopust, D., Vezys, V., Marzo, A.L. & Lefrancois, L. Preferential localization of effector memory cells in nonlymphoid tissue. *Science* **291**, 2413–2417 (2001).
4. Reinhardt, R.L., Khoruts, A., Merica, R., Zell, T. & Jenkins, M.K. Visualizing the generation of memory CD4 T cells in the whole body. *Nature* **410**, 101–105 (2001).
5. Manjunath, N. *et al.* Effector differentiation is not prerequisite for generation of memory cytotoxic T lymphocytes. *J. Clin. Invest.* **108**, 871–878 (2001).
6. Sallusto, F. & Lanzavecchia, A. Exploring pathways for memory T cell generation. *J. Clin. Invest.* **108**, 805–806 (2001).
7. Jameson, S.C. Maintaining the norm: T-cell homeostasis. *Nat. Rev. Immunol.* **2**, 547–556 (2002).
8. Busch, D.H., Pilip, I.M., Vijh, S. & Pamer, E.G. Coordinate regulation of complex T cell populations responding to bacterial infection. *Immunity* **8**, 353–362 (1998).
9. Kaech, S.M. & Ahmed, R. Memory CD8+ T cell differentiation: initial antigen encounter triggers a developmental program in naive cells. *Nat. Immunol.* **2**, 415–422 (2001).
10. Lau, L.L., Jamieson, B.D., Somasundaram, T. & Ahmed, R. Cytotoxic T-cell memory without antigen. *Nature* **369**, 648–652 (1994).
11. Murali-Krishna, K. *et al.* Counting antigen-specific CD8 T cells: a reevaluation of bystander activation during viral infection. *Immunity* **8**, 177–187 (1998).
12. Harrington, L.E., Galvan, M., Baum, L.G., Altman, J.D. & Ahmed, R. Differentiating between memory and effector CD8 T cells by altered expression of cell surface O-glycans. *J. Exp. Med.* **191**, 1241–1246 (2000).
13. Tussey, L., Speller, S., Gallimore, A. & Vessey, R. Functionally distinct CD8+ memory T cell subsets in persistent EBV infection are differentiated by migratory receptor expression. *Eur. J. Immunol.* **30**, 1823–1829 (2000).
14. Hislop, A.D. *et al.* EBV-specific CD8+ T cell memory: relationships between epitope specificity, cell phenotype, and immediate effector function. *J. Immunol.* **167**, 2019–2029 (2001).
15. Weninger, W., Crowley, M.A., Manjunath, N. & von Andrian, U.H. Migratory properties of naive, effector, and memory CD8(+) T cells. *J. Exp. Med.* **194**, 953–966 (2001).
16. Champagne, P. *et al.* Skewed maturation of memory HIV-specific CD8 T lymphocytes. *Nature* **410**, 106–111 (2001).
17. Unsoeld, H., Krautwald, S., Voehringer, D., Kunzendorf, U. & Pircher, H. Cutting edge: CCR7(+) and CCR7(-) memory T cells do not differ in immediate effector cell function. *J. Immunol.* **169**, 638–641 (2002).
18. Kunkel, E.J. & Butcher, E.C. Chemokines and the tissue-specific migration of lymphocytes. *Immunity* **16**, 1–4 (2002).
19. Ostler, T., Hussell, T., Surh, C.D., Openshaw, P. & Ehl, S. Long-term persistence and reactivation of T cell memory in the lung of mice infected with respiratory syncytial virus. *Eur. J. Immunol.* **31**, 2574–2582 (2001).
20. Mueller, S.N., Jones, C.M., Smith, C.M., Heath, W.R. & Carbone, F.R. Rapid cytotoxic T lymphocyte activation occurs in the draining lymph nodes after cutaneous herpes simplex virus infection as a result of early antigen presentation and not the presence of virus. *J. Exp. Med.* **195**, 651–656 (2002).
21. Norbury, C.C., Malide, D., Gibbs, J.S., Bennink, J.R. & Yewdell, J.W. Visualizing priming of virus-specific CD8+ T cells by infected dendritic cells *in vivo*. *Nat. Immunol.* **3**, 265–271 (2002).
22. Ahmed, R. & Gray, D. Immunological memory and protective immunity: understanding their relation. *Science* **272**, 54–60 (1996).
23. Fearon, D.T., Manders, P. & Wagner, S.D. Arrested differentiation, the self-renewing memory lymphocyte, and vaccination. *Science* **293**, 248–250 (2001).
24. Swain, S.L., Hu, H. & Huston, G. Class II-independent generation of CD4 memory T cells from effectors. *Science* **286**, 1381–1383 (1999).
25. Murali-Krishna, K. *et al.* Persistence of memory CD8 T cells in MHC class I-deficient mice. *Science* **286**, 1377–1381 (1999).
26. Tough, D.F., Borrow, P. & Sprent, J. Induction of bystander T cell proliferation by viruses and type I interferon in vivo. *Science* **272**, 1947–1950 (1996).
27. Tanchot, C., Lemonnier, F., Perarnau, B., Freitas, A. & Rocha, B. Differential requirements for survival and proliferation of CD8 naive or memory cells. *Science* **276**, 2057–2062 (1997).
28. Ku, C.C., Murakami, M., Sakamoto, A., Kappler, J. & Marrack, P. Control of homeostasis of CD8+ memory T cells by opposing cytokines. *Science* **288**, 675–678 (2000).
29. Schluns, K.S., Kieper, W.C., Jameson, S.C. & Lefrancois, L. Interleukin-7 mediates the homeostasis of naive and memory CD8 T cells *in vivo*. *Nat. Immunol.* **1**, 426–432 (2000).
30. Sprent, J. & Surh, C.D. Generation and maintenance of memory T cells. *Curr. Opin. Immunol.* **13**, 248–254 (2001).
31. Schluns, K.S., Williams, K., Ma, A., Zheng, X.X. & Lefrancois, L. Cutting edge: requirement for IL-15 in the generation of primary and memory antigen-specific CD8 T cells. *J. Immunol.* **168**, 4827–4831 (2002).
32. Becker, T.C. *et al.* Interleukin 15 is required for proliferative renewal of virus-specific memory CD8 T cells. *J. Exp. Med.* **195**, 1541–1548 (2002).
33. Kieper, W.C. *et al.* Overexpression of interleukin (IL)-7 leads to IL-15-independent generation of memory phenotype CD8+ T cells. *J. Exp. Med.* **195**, 1533–1539 (2002).
34. Tan, J.T. *et al.* Interleukin (IL)-15 and IL-7 jointly regulate homeostatic proliferation of memory phenotype CD8+ cells but are not required for memory phenotype CD4+ cells. *J. Exp. Med.* **195**, 1523–1532 (2002).
35. Goldrath, A.W. *et al.* Cytokine requirements for acute and basal homeostatic proliferation of naive and memory CD8+ T cells. *J. Exp. Med.* **195**, 1515–1522 (2002).
36. Razvi, E., Welsh, R. & McFarland, H. In vivo state of antiviral CTL precursors. *J. Immunol.* **154**, 620–632 (1995).
37. Hamann, D. *et al.* Phenotypic and functional separation of memory and effector human CD8+ T cells. *J. Exp. Med.* **9**, 1407–1418 (1997).
38. Jacob, J. & Baltimore, D. Modelling T-cell memory by genetic marking of memory T cells *in vivo*. *Nature* **399**, 593–597 (1999).
39. Opferman, J.T., Ober, B.T. & Ashton-Rickardt, P.G. Linear differentiation of cytotoxic effectors into memory T lymphocytes. *Science* **283**, 1745–1748 (1999).
40. Lauvau, G. *et al.* Priming of memory but not effector CD8 T cells by a killed bacterial vaccine. *Science* **294**, 1735–1739 (2001).
41. Tomiyama, H., Matsuda, T. & Takiguchi, M. Differentiation of human CD8(+) T cells from a memory to memory/effector phenotype. *J. Immunol.* **168**, 5538–5550 (2002).
42. Wong, P. & Pamer, E.G. Cutting edge: antigen-independent CD8 T cell proliferation. *J. Immunol.* **166**, 5864–5868 (2001).
43. van Stipdonk, M.J., Lemmens, E.E. & Schoenberger, S.P. Naive CTLs require a single brief period of antigenic stimulation for clonal expansion and differentiation. *Nat. Immunol.* **2**, 423–429 (2001).
44. Kaech, S.M., Hemby, S., Kersh, E. & Ahmed, R. Molecular and functional profiling of memory CD8 T cell differentiation. *Cell* **111**, 837–851 (2002).
45. Bradley, L.M., Watson, S.R. & Swain, S.L. Entry of naive CD4 T cells into peripheral lymph nodes requires L-selectin. *J. Exp. Med.* **180**, 2401–2406 (1994).
46. Arbones, M.L. *et al.* Lymphocyte homing and leukocyte rolling and migration are impaired in L-selectin-deficient mice. *Immunity* **1**, 247–260 (1994).
47. Campbell, J.J. *et al.* CCR7 expression and memory T cell diversity in humans. *J. Immunol.* **166**, 877–884 (2001).
48. Iezzi, G., Scheidegger, D. & Lanzavecchia, A. Migration and function of antigen-primed nonpolarized T lymphocytes in vivo. *J. Exp. Med.* **193**, 987–993 (2001).
49. Appay, V. *et al.* Memory CD8+ T cells vary in differentiation phenotype in different persistent virus infections. *Nat. Med.* **8**, 379–385 (2002).
50. Wills, M.R. *et al.* Identification of naive or antigen-experienced human CD8(+) T cells by expression of costimulation and chemokine receptors: analysis of the human cytomegalovirus-specific CD8(+) T cell response. *J. Immunol.* **168**, 5455–5464 (2002).
51. Moskophidis, D., Lechner, F., Pircher, H. & Zinkernagel, R.M. Virus persistence in acutely infected immunocompetent mice by exhaustion of antiviral cytotoxic effector T cells. *Nature* **362**, 758–761 (1993).
52. Zajac, A.J. *et al.* Viral immune evasion due to persistence of activated T cells without effector function. *J. Exp. Med.* **188**, 2205–2213 (1998).
53. Banchereau, J. & Steinman, R.M. Dendritic cells and the control of immunity. *Nature* **392**, 245–252 (1998).
54. Migueles, S.A. *et al.* HIV-specific CD8+ T cell proliferation is coupled to perforin expression and is maintained in nonprogressors. *Nat. Immunol.* **3**, 1061–1068 (2002).
55. Harrington, L.E., van der Most, R.G., Whitton, J.L. & Ahmed, R. Recombinant vaccinia virus-induced T-cell immunity: quantitation of the response to the virus vector and the foreign epitope. *J. Virol.* **76**, 3329–3337 (2002).
56. Laouar, Y. & Crispe, I.N. Functional flexibility in T cells: independent regulation of CD4+ T cell proliferation and effector function in vivo. *Immunity* **13**, 291–301 (2000).